Measurements of Pressure and Thermal Wakes in a Transonic Turbine Cascade

by

Alexis Mezynski

Thesis submitted to the Faculty of the
Virginia Polytechnic Institute and State University
in partial fulfillment of the requirements for the degree of

Master of Science

in

Mechanical Engineering

APPROVED:

Dr. Thomas E. Diller, Co-Chairman

Dr. Wing F. Ng, Co-Chairman

Dr. Tibor Kiss

August 1994

Blacksburg, Virginia

MEASUREMENTS OF PRESSURE AND THERMAL WAKES IN A TRANSONIC TURBINE CASCADE

by

Alexis Mezynski

Dr. T.E. Diller and Dr. W.F. Ng, Co-Chairmen

Mechanical Engineering

(ABSTRACT)

The effects of freestream turbulence on the total pressure and total temperature in the wake of a cooled transonic turbine cascade with heated flow are presented in this thesis. The experiment was conducted in the Virginia Tech Cascade Wind Tunnel. A dual hot wire aspirating probe was used to make high frequency, unsteady total pressure and temperature measurements. The probe design was modified to be used in a high temperature environment. The flow was heated to temperatures exceeding 140°C and the turbine blades were actively cooled using gaseous nitrogen to maintain a gas to blade temperature ratio between 1.3 and 1.4. A turbulence screen was used to change the freestream turbulence from 3.3% to 7.5%. Mean and turbulent total pressure and temperature quantities are presented. The higher freestream turbulence resulted in lower total pressure and total

temperature turbulence intensities in the wakes of the turbine blades. The freestream turbulence level had no measurable effect on the blade losses.

Abstract

Acknowledgments

Without the help from others, the completion of this thesis would not be possible. I would first and foremost like to thank D. J. Osborne for all of his assistance in building and calibrating the probe. I do appreciate the many hours you spent replacing hot wires.

Second, I wish to thank my co-advisors Dr. T.E. Diller and Dr. W.F. Ng. Without their guidance, I would have never been able to complete this work on time.

Appreciation is also expressed to the other members of the design team: Tibor Kiss, Terry Reid, and Loren Johnson. Their knowledge and labor immeasurably contributed to the collection and understanding of the data presented.

Finally, I wish to express my gratitude to my wife, who has endured the many hours I've spent at the wind tunnel and working on my computer.

Table of Contents

List of Figures

List of Tables

Nomenclature

a	calibration constant
A	area
b	calibration constant
C	calibration parameter
C_p	specific heat at constant pressure
d	hot wire diameter
D	calibration parameter
h	heat transfer coefficient
k	thermal conductivity of air
l	length of hot wire
m	calibration constant
$\dot{m}$	massflow rate
M	Mach number
P	pressure
q	heat transfer rate
r	recovery factor
R	resistance
$\Re$	gas constant

T	temperature, turbulence intensity
V	anemometer bridge voltage

GREEK LETTERS

α	thermal diffusivity of hot wire
γ	ratio of specific heats for air
μ	absolute viscosity of air
π	pi (3.14159265)
ρ	density of air

SUBSCRIPTS

1	first hot wire
2	second hot wire
c	cross-sectional, cold
e	environment
h	hot
i	index for each hot wire
m	mean
ref	reference
s	series
t	refers to total property
u	velocity
w	wire
∞	infinity

SUPERSCRIPTS

*	refers to property at throat
-	averaged variable
'	fluctuating component

ACRONYMS AND ABBREVIATIONS

AC	fluctuating quantity
ASME	American Society of Mechanical Engineers
BASIC	computer language
C	Celsius
DC	mean quantity
Hz	hertz
IBM PC	International Business Machines Personal Computer
K	Kelvin
kHz	kilohertz
LVDT	Linear Variable Displacement Transducer
MIT	Massachusetts Institute of Technology
ms	milliseconds
Pa	Pascal
psig	pounds per square inch, gage
RMS	root-mean-square
TK	computer software
VPI	Virginia Polytechnic Institute and State University

1.0 Introduction

With the continuing drive to design more efficient and reliable gas turbine engines, there is a current interest in understanding the flow characteristics in the turbine section. The overall objective of this thesis is to better understand the exit flow from a transonic turbine stage. If this flowfield is known, then subsequent stages can be designed using this information resulting in better performance and reliability.

Specifically researched in this thesis is the influence of freestream turbulence on the aerodynamic and thermodynamic properties of the flow downstream of a turbine cascade. A dual hot wire aspirating probe was used to measure the total pressure and total temperature of the flow. This probe can detect high frequency fluctuations in the total temperature and total pressure while traversing through several blade passages. The experiment was conducted in a transonic cascade wind tunnel with heated flow and cooled turbine blades. This study is preliminary in nature and was intended to test a new configuration of the aspirating probe as well as collect the total pressure and total temperature data. The aspirating probe was modified for use in a high temperature environment.

Several dual hot wire aspirating probes have been used to measure flow characteristics downstream of compressor cascades. Initial development of the aspirating probe was accomplished by Ng and Epstein at MIT in the early 1980's [1]. Later, Ng used an aspirating probe to measure total temperature and pressure in the shed vortex sheet of a circular cylinder, to measure turbulence intensity in a transonic cryogenic wind tunnel, and to measure flow properties downstream of a transonic compressor [2]. Osborne utilized a similar aspirating probe to measure the flowfield behind a transonic compressor [3]. The probe has also been used by Ninneman to measure concentration levels in supersonic air/helium shear layers [4]. These probes all used platinum-tungsten hot wires. Van Zante et al switched to platinum-iridium wires to be used in measuring flow downstream of a compressor rotor [5]. By doing this, higher wire operating temperatures were used, resulting in better data reduction accuracy. These platinum-iridium hot wires were also used on the probe in this experiment. The higher wire operating temperatures were necessary due to the higher flow temperatures present in this research.

The effect of freestream turbulence on heat transfer is well documented. Higher freestream turbulence levels result in increased heat transfer rates. Moss and Oldfield researched the effect of turbulence on heat flux into a flat plate [6]. Gundappa and Diller investigated the effect of different mesh sizes and grid spacing on the freestream turbulence and heat transfer into a circular cylinder [7]. Glezer et al looked at the relationship between freestream turbulence and heat transfer to a turbine airfoil [8]. The effect of turbulence on heat transfer into a linear turbine cascade was the

focus of a study by Maciejewski and Rivir [9]. Freestream turbulence effects on the flow properties downstream of a turbine cascade is the main area explored by this thesis.

The aspirating probe is used to measure total pressure and temperature fluctuations downstream of a cooled turbine cascade. The research which this thesis documents was conducted in a higher temperature environment than the probe has previously been subjected to. The transonic flow is heated to temperatures exceeding 140°C. The effects of turbulence on the probe measurements were also explored. Temperature and pressure turbulence intensities were calculated and with data from other instrumentation, total heat transfer into the blades and losses through the blade passages were obtained. The author is not aware of any exit flow studies accomplished in a cooled turbine cascade with heated flow. It is emphasized that these are preliminary measurements and further studies will follow in the future.

The following chapter will provide a description of the facility used for the experiment and the characteristics of the test section. Chapter 3 goes more in depth on the actual experiment. It provides details of the probe design and calibration, the hot wire's operating principles, and the data acquisition systems used. Chapter 4 describes how the data from the calibration and the tunnel runs was reduced. Chapter 5 presents the results of the experiment and a discussion of these results. Finally, Chapter 6 provides a summary of conclusions and areas for future exploration.

2.0 Experimental Facility

This chapter provides an overview of the facility used to conduct this experiment. Specifically discussed are the wind tunnel characteristics and operation procedure and the attributes of the test section.

2.1 Wind Tunnel

The experiments were conducted in the Virginia Polytechnic Institute Cascade Wind Tunnel. It is a blow-down wind tunnel which provides up to 30 second run times. Compressed air is run through dryers to remove moisture from the flow and is then stored in a reservoir. The flow then goes through a valve which controls the tunnel pressure. A BASIC program on an IBM PC controls the actuation schedule of the valve based on feedback it is receiving from a pressure transducer measuring the flow's total pressure upstream of the cascade. This actuation ensures a relatively constant tunnel pressure during a tunnel run. More details on the valve control can be found in Bertsch [10].

The cascade tunnel also has a heating loop which allows for heated runs (See Figure 2-1). In between runs, one valve is closed and one valve is

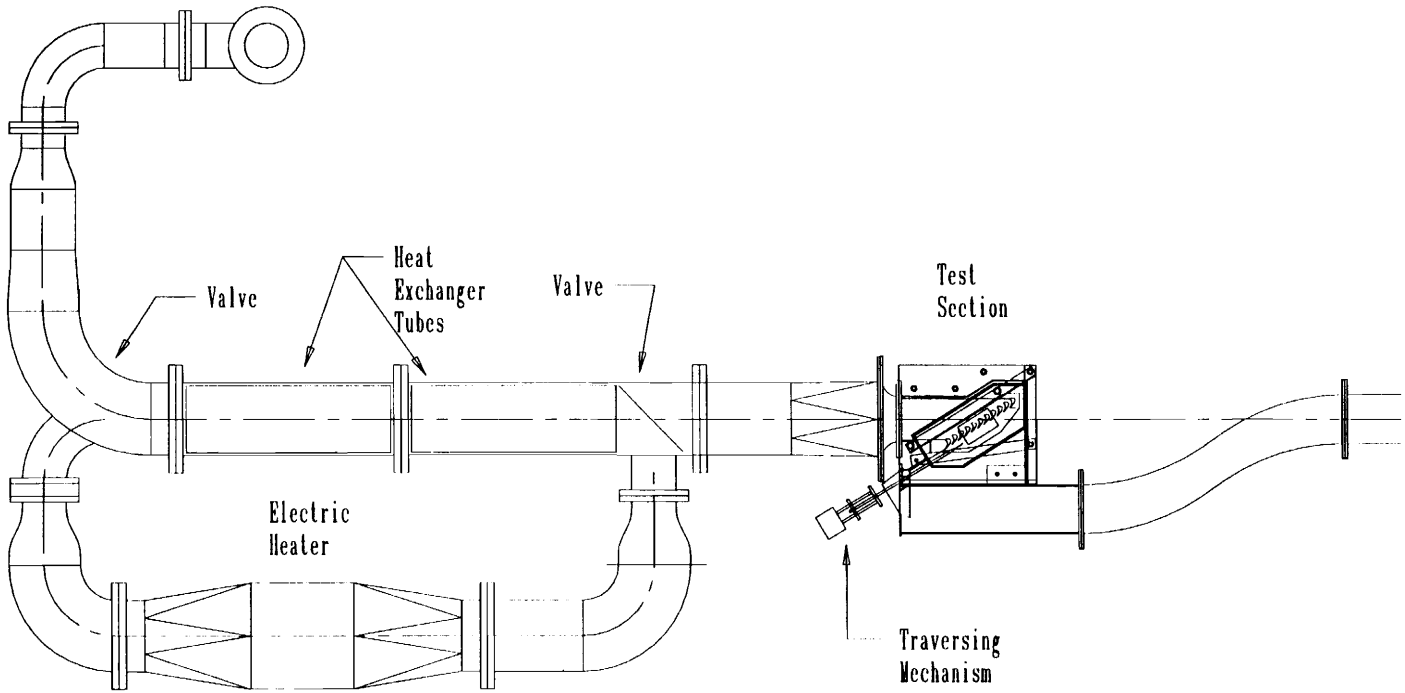

Figure 2-1 VPI Cascade Wind Tunnel Facility

opened to form the heating loop. The electric heater is turned on and an axial fan drives air through the heating loop. The heat is stored in 250 kg of copper tubes. These tubes are 1.59 cm in diameter and 1 m long. The tube temperature is monitored by a surface mounted thermocouple, and the hot gas temperature is monitored with an air probe thermocouple. It takes approximately 45 minutes to initially heat the tubes to a temperature of 180°C. Subsequent heatings require between five and ten minutes. After the tubes meet the desired temperature, the electric heater is shut off, but the fan is allowed to run for another five minutes to equalize the tube temperatures. After the fan is shut off, one valve is opened and the other is closed, and the tunnel is operated. The tubes then transfer their thermal energy to the flow. Flow temperatures of over 140°C can be achieved by using this loop. After exiting the heating tubes, the flow passes through a circular to rectangular transition piece and enters the test section.

For supersonic exit Mach numbers, the flow enters the test section at Mach 0.36. The design average isentropic exit Mach number is 1.26. For some of the runs, a turbulence screen was placed directly upstream of the test section to increase the turbulence level of the flow. The mesh size was 12.5 mm by 12.5 mm with a thickness of 2 mm. A TSI bare hot wire probe was placed upstream of the test section to measure the freestream turbulence levels. The turbulence screen increased the freestream turbulence from 3.3% to 7.5% [11].

2.2 The Cascade

The cascade consists of an eleven turbine blades, two end-blocks, and two Plexiglas side plates (see Figure 2-2). These plates allow for optical information to be gathered. The blades are two inches in span and have a 1.8 inch aerodynamic chord with a blade spacing of 1.5 inches. The cascade is placed in the test section of the cascade tunnel and secured. The three center blades are cooled by pumping gaseous nitrogen through a horseshoe shaped cooling channel. During a run, the flow temperature slowly decreases as the heat exchanger tubes lose their thermal energy. However, the blades also get cooler due to the nitrogen cooling loops. Therefore, gas to blade temperature ratios between 1.3 and 1.4 can be maintained throughout the runs.

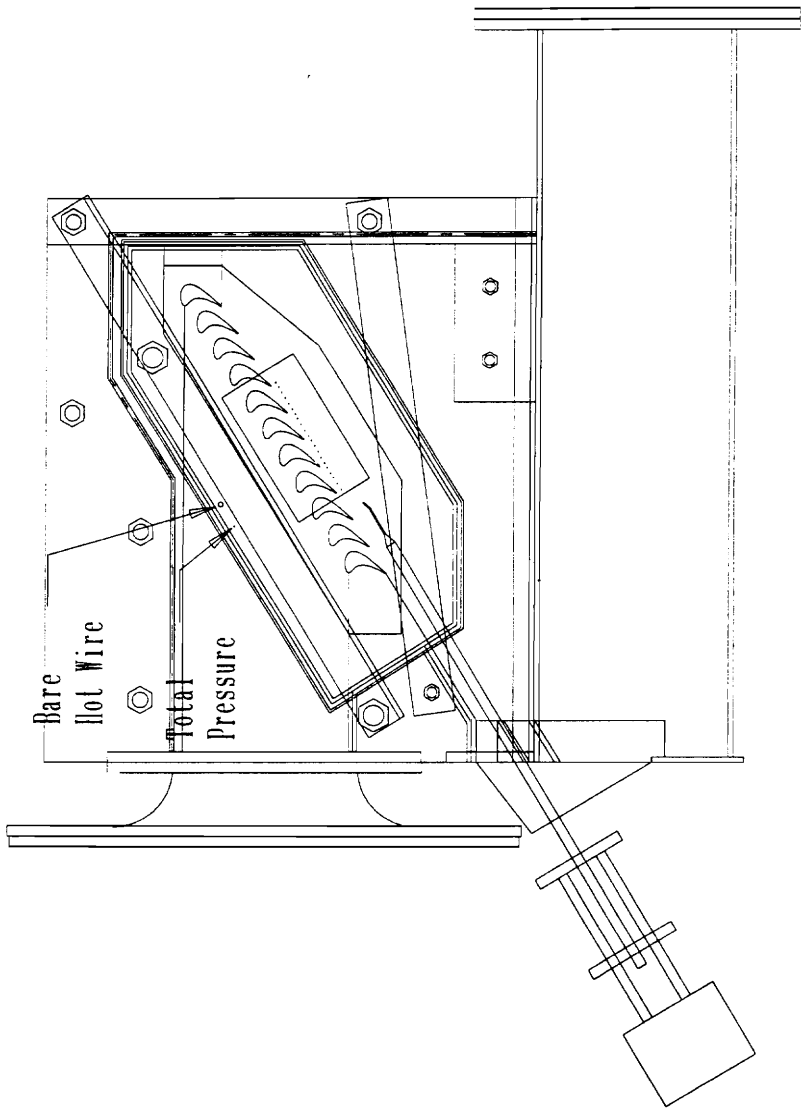

Figure 2-2 Test Section

3.0 The Experiment

This chapter describes the instrumentation used in the experiment. Specifically discussed are the probe design and operating principles, the probe calibration, the traversing mechanism, and the data acquisition system.

3.1 The Probe

The probe is a dual hot wire aspirating probe based on a similar probe by Ng and Epstein [1] with modifications like those made by Van Zante et al [5]. The probe is unique in that it is possible to obtain high frequency, unsteady total pressure and total temperature measurements in a high speed flow.

3.1.1 Probe Design

A schematic of the aspirating probe head is presented in Figure 3-1. The aspirating part of the probe has two 12.7μm diameter, platinum-iridium, coplanar hot wires mounted to brass supports insulated by epoxy. The hot

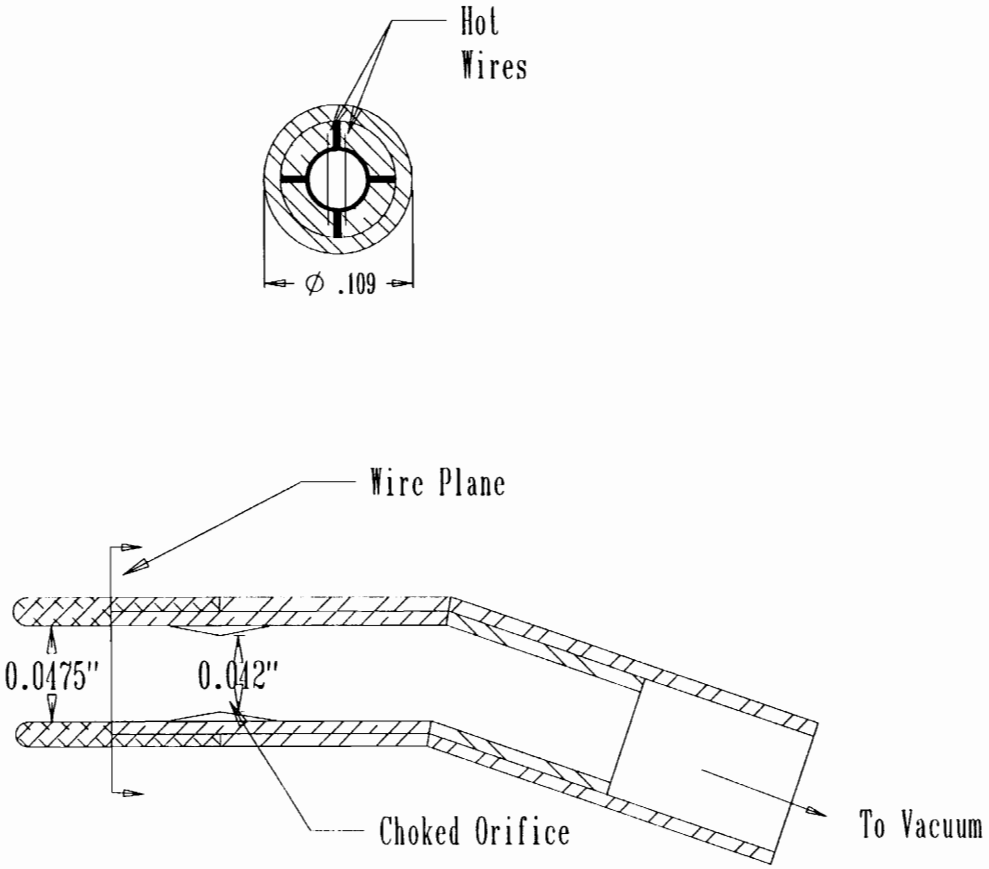

Figure 3-1 Aspirating Probe Head

wires have different overheat ratios and operate on separate constant temperature anemometer circuits. They are also copper coated at their ends to minimize the boundary layer interference effects. The choking orifice has a diameter of 0.042" while the channel diameter is 0.0475". The orifice is kept choked by attaching a vacuum line to the probe. The pressure in the vacuum line is always sufficiently low to ensure choking at the wire plane. This results in a constant Mach number of 0.55 through the wire plane of the aspirating probe. To allow for easy replacement of broken wires, a removable aluminum probe cap is attached in front of the hot wires . To ensure that the flow enters normal to the wire plane, the probe head is aligned parallel to the exit flow of the cascade.

The probe is twenty-nine inches long so that it can make measurements behind the three cooled center blades. The six inch probe stem is surrounded by a steel diamond sheath (See Figure 3-2). This sheath provides added structural support and minimized the probe vibration and blockage when flow was present. All of the joints were adhered with aerospace structural epoxy. This epoxy was used due to its high strength and its temperature resistance capability.

A high frequency response Kulite Model XCQ-062-50A pressure transducer is mounted adjacent to the aspirating part of the probe. The presence of this transducer allows for another means of determining the total pressure of the flow without relying on the hot wire data.

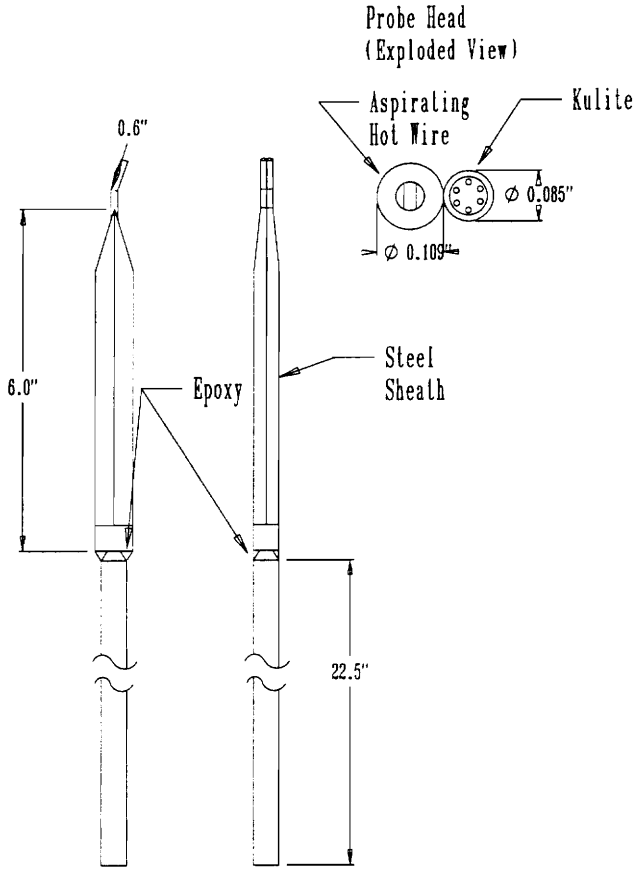

Figure 3-2 Dual Hot Wire Aspirating Probe

To minimize the chance of any other foreign particles resulting in damage to the hot wires, the aspirating line was operated only while the probe was traversing.

3.1.2 Principle of Operation

Because the flow is choked through the orifice, the anemometer bridge circuit voltage is sensitive only to the temperature difference between the wire and the fluid and to the mass flux through the wire plane [12]. For a constant temperature hot wire, with a fluid of uniform composition, the wire voltage of the anemometer bridge circuit is as follows:

$$V^2 = \frac{(R_s + R_w)^2}{R_w} \times \pi \cdot lk \left\{ a \left[\frac{d}{\mu} \frac{P_T}{\sqrt{T_T}} \frac{A^*}{A_c} \sqrt{\frac{\gamma}{\Re}} \left(\frac{2}{\gamma + 1} \right)^{(\gamma+1)/2(\gamma-1)} \right]^m + b \right\} (T_w - rT_T) \tag{3.1}$$

where R_W is the resistance of the hot wire while operating, R_S is the bridge resistance in series with the wire, l is the hot wire length, and k is the thermal conductivity of the fluid. μ is the fluid viscosity, d is the wire diameter, A/A^* is the channel to sonic orifice area ratio, $\Re$ is the gas constant, and γ is the ratio of specific heats. P_t and T_t are the fluid total pressure and temperature, respectively. r is the recovery factor and T_W is the wire operating temperature. The constants a, b, and m are empirically derived from the Collis and Williams equation for Nu [12]. There is a separate voltage

expression for each wire. Once the probe geometry, wire type, and fluid type are chosen, the equation can be collapsed to the following form [2]:

$$\frac{V_i^2}{\left(T_{w_i} - rT_T\right)} = C_i\left(\frac{P_T}{\sqrt{T_T}}\right)^{m_i} + D_i \qquad (3.2)$$

In previous work, it was assumed that C, D, and m were constants and could be determined from calibration. However, Kotidis [12] and Van Zante et al [5] discovered that C and D were functions of the fluid temperature. T_W was then determined after setting the overheat ratio by evaluating the following expression:

$$OHR_i = \frac{R_{h_i}}{R_{c_i}} = 1 + \alpha\left(T_{w_i} - T_e\right) \qquad (3.3)$$

where OHR is the overheat ratio, R_h is the operating resistance of the hot wire, R_c is the resistance of the hot wire at the environment temperature, T_e is the environment temperature and α is the temperature coefficient of resistance of the hot wire. Previous analyses [2], [5] assumed that α was constant. However, Kotidis [12] discovered that α varied with temperature, thus making T_W an additional unknown. For each hot wire, $C(T_m)$, $D(T_m)$, m, and T_w can be determined from the calibration data.

3.1.3 Calibration Procedure

For this experiment, the hot wires had to be calibrated to a temperature of 160°C and a pressure of 25 psig. To accomplish this task, a calibration tank was used [see Figure 3-3]. Two drum heaters were wrapped around the tank which was insulated so that steady state conditions could be reached. As was previously mentioned, C and D were determined to be functions of temperature. There are two ways to deal with this observation: 1) do a detailed calibration for each fluid temperature and determine C and D from a curve fit [6], or 2) determine a functional relationship between C, D, and the fluid temperature. Kotidis [12] derived these functional relationships:

$$C = C_{ref}\frac{k}{k_{ref}}\left[\frac{\mu_{ref}\left(\frac{\gamma}{\Re}\right)^{1/2}\left(\frac{2}{\gamma+1}\right)^{\frac{\gamma+1}{2(\gamma-1)}}}{\mu\left(\frac{\gamma_{ref}}{\Re}\right)^{1/2}\left(\frac{2}{\gamma_{ref}+1}\right)^{\frac{\gamma_{ref}+1}{2(\gamma_{ref}-1)}}}\right]^{m}\left[\frac{\frac{T_m}{T_\infty}}{\left(\frac{T_m}{T_\infty}\right)_{ref}}\right]^{0.17} \tag{3.4}$$

$$D = D_{ref}\frac{k}{k_{ref}}\left[\frac{\frac{T_m}{T_\infty}}{\left(\frac{T_m}{T_\infty}\right)_{ref}}\right]^{0.17} \tag{3.5}$$

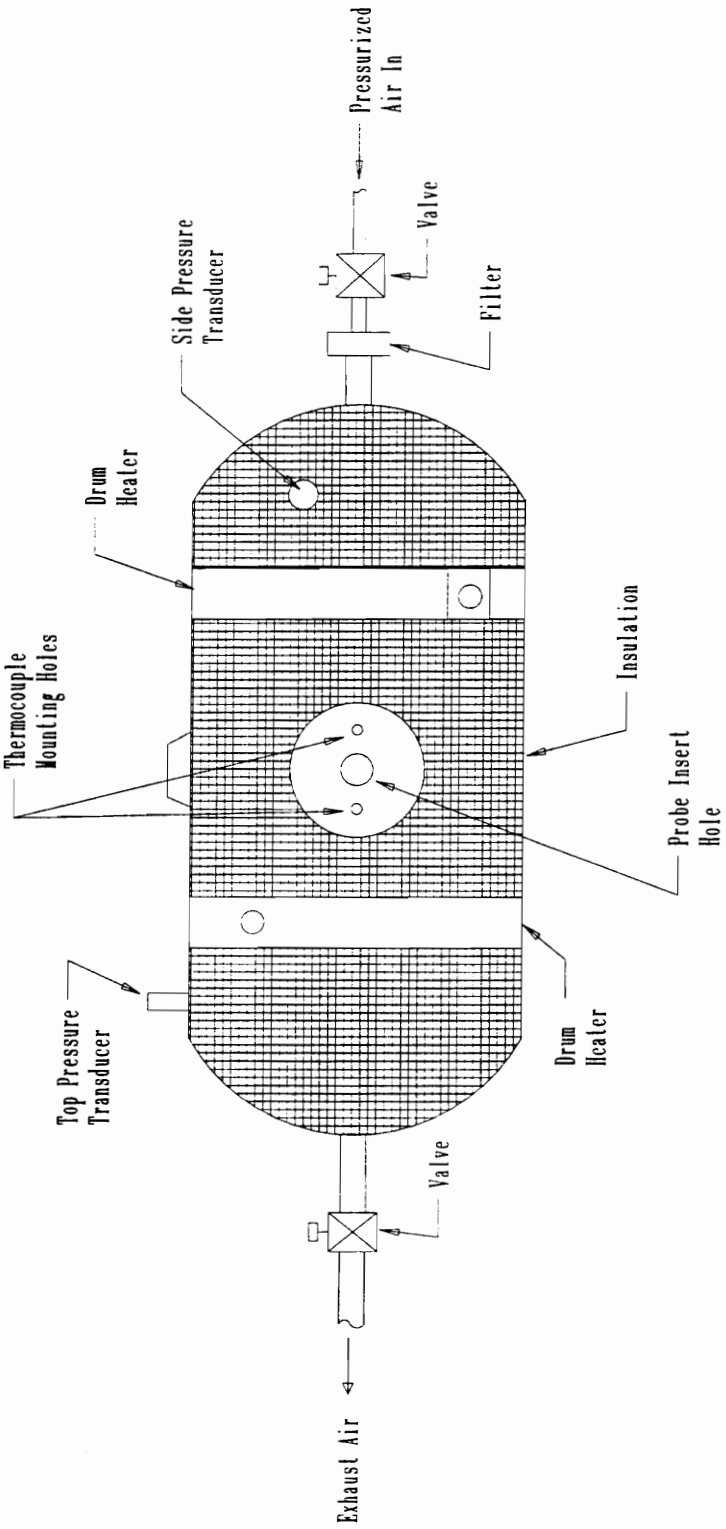

Figure 3-3 Calibration Tank

where C_{ref} and D_{ref} are curve fit constants determined from a room temperature calibration, k_{ref} and γ_{ref} are the fluid thermal conductivity and ratio of specific heats evaluated at the reference "film temperature". The "film temperature" is the arithmetic mean of the freestream static temperature and the wire operating temperature. By using Equation 3.4 and 3.5, the calibration may be accomplished by using several "random conditions" rather than a full scale calibration at each temperature.

A difficulty arises, however, in evaluating the flow properties at the "film temperature." In order to calculate the film temperature, the static temperature must be known. If the total temperature and the Mach number are known, then the static temperature can be found, but γ is evaluated at the "film temperature." Therefore an iterative technique must be used. Also, T_w is not known and must also iterated upon to find which value yields the least amount of error over the entire calibration space. Table 3-1 lays out the calibration space.

For this calibration overheat ratios of 1.28 and 1.38 were used for wire 1 and wire 2, respectively. These overheat ratios allowed a sufficient difference between the two hot wire temperatures and also between the wire and freestream temperature. If the differences are not great enough, the hot wire calibration space is too small. If the overheats are too high, the wires age quickly. The reference calibration was taken at sixteen different pressures and thirty-two other "random conditions" were used. The hot wire and Kulite signals were sampled at 20 kHz and the pressure transducer signals were sampled at 50 Hz. All signals were averaged over the 0.8

Table 3-1

Calibration Space

	Reference		Heated		Heated	
Point #	Tempera ture	Pressure	Tempera ture	Pressure	Tempera ture	Pressure
1	25 C	25 psi	50 C	25 psi	140 C	25 psi
2	25	23.5	50	15	140	15
3	25	22	50	5	140	5
4	25	20.5	100	25	150	25
5	25	19	100	15	150	15
6	25	17.5	100	5	150	5
7	25	16	110	25	160	25
8	25	14.5	110	15	160	22.5
9	25	13	110	5	160	20
10	25	11.5	120	25	160	17.5
11	25	10	120	15	160	15
12	25	8	120	5	160	12.5
13	25	6	130	25	160	10
14	25	4	130	15	160	7.5
15	25	2	130	10	160	5
16	25	0	130	5	160	2.5

seconds which they were sampled over. The hot wire calibration space is shown in Figure 3-4.

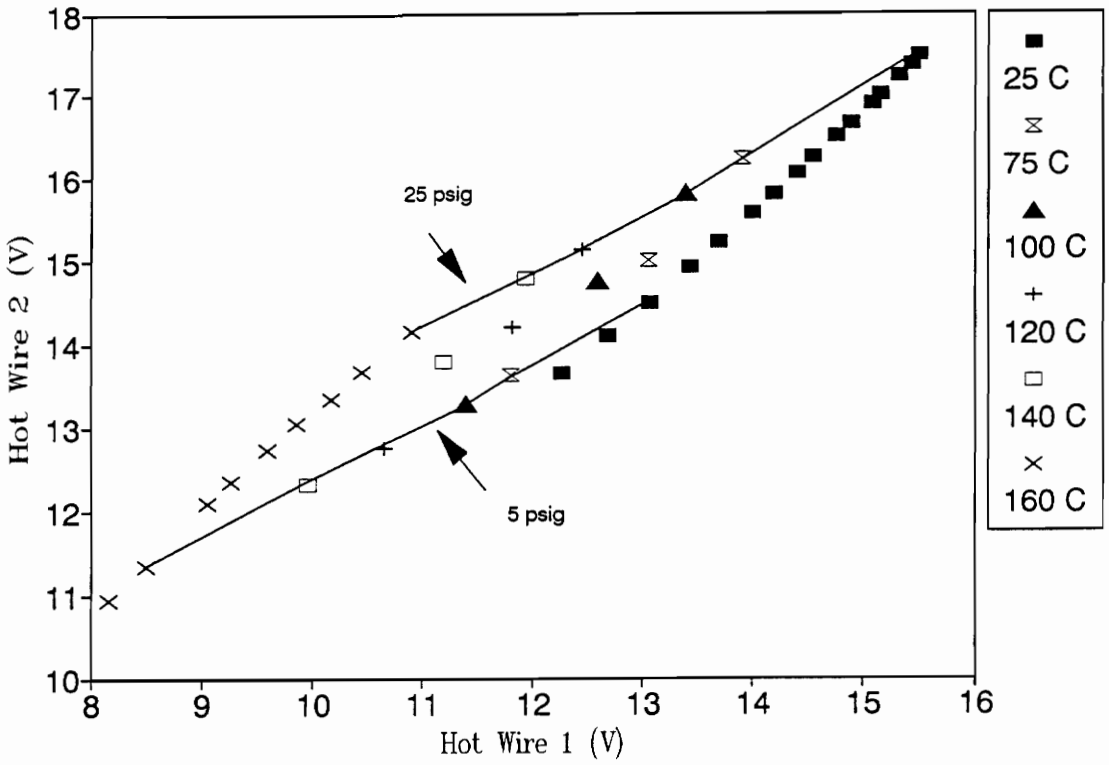

Figure 3-4 Hot Wire Calibration Space

3.2 Traversing Mechanism

The traversing mechanism contains a stepper motor which drives the rack. The half inch diameter probe body is attached to the rack and is able to move parallel to the blade row, 3/8" downstream of the blades. To control the traverse, a BASIC code was written for an IBM PC. This code controls the distance the traverse moves as well as its speed. For this experiment the probe traverses three inches (two blade passages) in ten seconds.

The position of the probe is recorded by using a Linear Variable Displacement Transducer. The voltage output from this transducer can be converted to a displacement. Therefore, the position of the probe with respect to the cascade is known at all times during the experiment.

3.3 Data Acquisition

Data acquisition schematics for the taking of the calibration data and the tunnel run data are shown in Figures 3-5 and 3-6, respectively. Because they are similar, only the procedure for tunnel runs is described in detail below.

The hot wires are controlled by two separate anemometers. The anemometers include the DANTEC Type 55M01 Main Unit and the DANTEC Type 55M10 CTA Standard Bridge. The bridge output voltages for the hot wire signals then pass through an offset amplifier and a low pass filter before entering the LeCroy 6810 Waveform Recorder. The LeCroy is

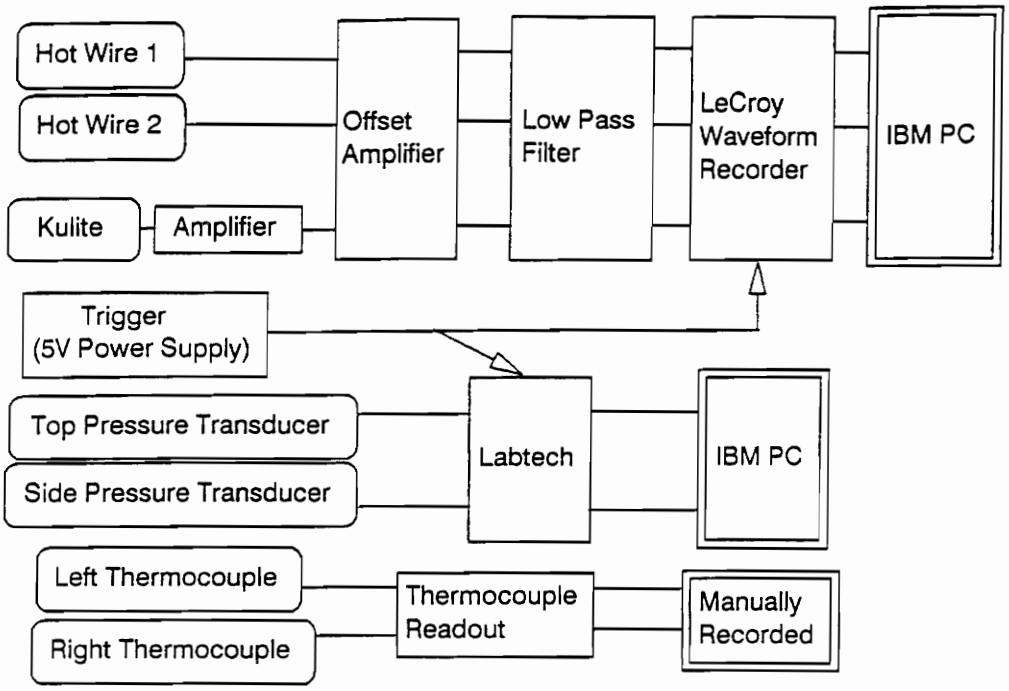

Figure 3-5 Calibration Data Acquisition

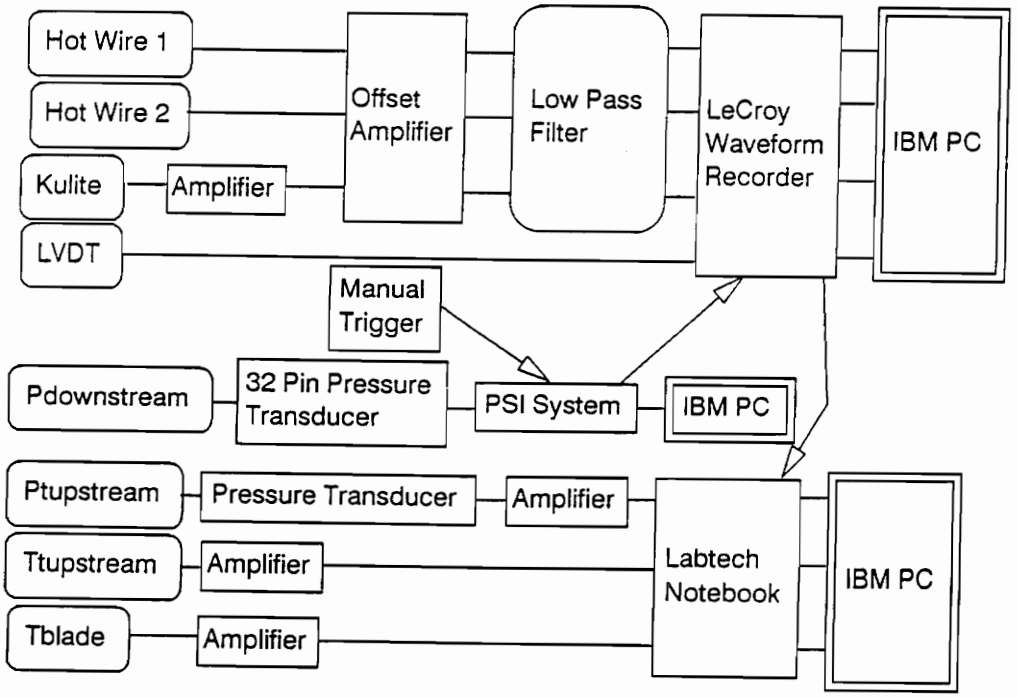

Figure 3-6 Tunnel Run Data Acquisition

a high speed analog to digital converter which stores the data in its large memory. After the runs, the data is downloaded to an IBM PC. The DC voltage levels are monitored with two voltmeters and the AC levels are monitored on an oscilloscope.

The Kulite pressure transducer signal is first conditioned by a National Instruments 2310 Signal Conditioning Amplifier where the signal is amplified by a factor of one hundred. The signal then passes through the offset amplifier and the low pass filter and enters the LeCroy. The Kulite data is also stored on the IBM PC and Kulite data was stored on another IBM PC.

The purpose of the offset amplifier is to maximize the analog to digital resolution of the LeCroy. Wire 1, wire 2, and the Kulite voltages were offset by eleven, fourteen, and three volts, respectively. The LeCroy is able to take high frequency measurements on up to eight channels at a time. For this experiment, it sampled at a rate of 20 kHz and stored the 12.5 seconds worth of data (256,000 data points per signal) on an IBM PC.

The LVDT voltage was recorded on the LeCroy while the blade temperature, upstream flow temperature, and upstream flow pressure were all recorded using Labtech Notebook. This data was sampled at 20 Hz. The blade and flow temperatures were measured by Type K thermocouples 5 mils in diameter. The flow total pressure was taken as a pitot measurement converted to a voltage by a pressure transducer.

The static pressure 1/4" downstream of the blades was also recorded for each run by using the PSI Pressure Systems model 780B. Twenty-one static pressure taps mounted on the Plexiglas endwalls and a total pressure

tap mounted on the aluminum door were connected to a thirty-two channel pressure transducer (model ESP-32). This transducer's signal was received by the PSI system and stored on an IBM PC.

The BASIC program which sets up for taking the static pressure data also controls the traverse. The program is manually triggered when the tunnel pressure levels out causing the traverse to start moving and the PSI system to begin taking data. The PSI system also sends a trigger to the LeCroy which starts taking hot wire, Kulite, and LVDT data. The LeCroy in turn sends a trigger to Labtech Notebook which starts taking upstream pressure and temperature data as well as blade temperature data.

4.0 Data Reduction

This chapter discusses how the hot wire data was reduced as well as how to reduce the data with the Kulite transducer and one hot wire.

4.1 Hot Wire Reduction

The hot wire calibration data was first reduced to determine the wire temperatures and the calibration constants. By using this information, the hot wire voltages could then be converted into total pressures and temperatures for tunnel run data.

4.1.1 Calibration

Calibration data was taken for sixteen pressures ranging from 0 to 25 psig at room temperature. These were the "reference" conditions. The 32 other calibration points were at various pressures at temperatures ranging from 50 to 160°C. The first task in the calibration data reduction was to determine the wire operating temperatures (See Figure 4-1). Using several

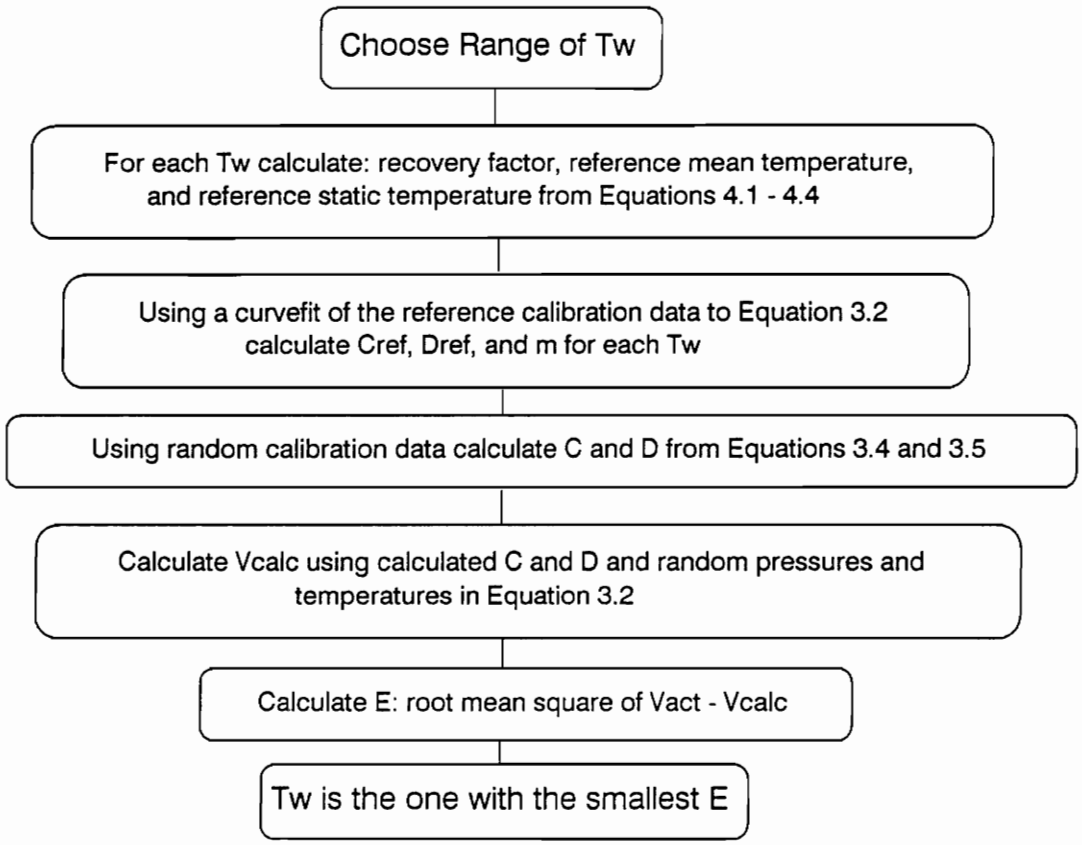

Figure 4-1 Determination of T_W

TK Solver programs, this was accomplished. First, the raw hot wire data had their offsets added back on. Then, for a given range of wire temperatures, the recovery factor, the reference mean temperature, and the reference static temperature were calculated by solving the following equations:

$$\left(\frac{A}{A^*}\right)^2 = \frac{1}{M^2}\left[\frac{2}{\gamma+1}\left(1+\frac{\gamma-1}{2}M^2\right)\right]^{\frac{\gamma+1}{\gamma-1}} \tag{4.1}$$

$$\frac{T_\infty}{T_t} = \left(1+\frac{\gamma-1}{2}M^2\right)^{-1} \tag{4.2}$$

$$T_m = \frac{T_\infty + T_w}{2} \tag{4.3}$$

$$r = \frac{T_\infty}{T_t} \tag{4.4}$$

γ was allowed to vary with T_m. Next, for each wire temperature, a curve fit to Equation 3.2 was accomplished using the reference data. Now, C_{ref}, D_{ref}, and m are known for each wire temperature. Using the reference constants, and the reference temperatures, the voltage output is calculated for the 32 random conditions by using Equations 3.4, 3.5, and 3.2. All thermal properties of the flow were allowed to vary with T_m. This voltage was subtracted from the actual voltage to generate a list of errors. For each wire temperature, the list of errors was squared, summed, and then square rooted. The wire temperature with the least mean squared error is the actual wire

temperature. For this wire temperature, all the reference parameters are known and are now fixed for the flow data reduction. The results are summarized in Table 4-1.

Table 4-1

Calibration Parameters

	First Wire Set	
	Wire 1	Wire 2
T_w (K)	**501**	**650**
OHR	**1.28**	**1.38**
C_{ref}	**0.00020**	**0.000101**
m	**0.834**	**0.889**
D_{ref}	**0.627**	**0.512**
T_{mref} (K)	**393.6**	**463.7**
$T_{\infty ref}$ (K)	**277.2**	**277.4**

4.1.2 Flow Data Reduction

When reducing the data using both hot wires, the two hot wire voltages and the reference parameters are known for each hot wire. Therefore, Equations 3.2, 3.4, and 3.5 can be written for each hot wire. Once again, the thermal properties are assumed to be functions of T_m. Since there are six equations and six unknowns (T_t, P_t, C_1, C_2, D_1, and D_2), they can be solved simultaneously. TK Solver was the tool used to accomplish this task. The

uncertainty for the pressure measurements is 323 Pa and for the temperature measurements is 0.26°C.

4.2 Kulite Data Reduction

Since the Kulite pressure transducer voltage was also recorded during the calibration procedure, a linear fit can be accomplished to determine the pressure from the voltage. This linear fit can then be used to find the total pressure from the flow data. Then, only one wire's output signal is needed to determine the total temperature of the flow.

4.3 Turbulence Intensities

Turbulence intensity is a way to quantify the fluctuating properties in the flow. It can be calculated for any parameter by taking the root mean square (RMS) of the fluctuating part of the signal and dividing by the signal mean. The total temperature and total pressure turbulence intensities are calculated from the hot wire results using Equations 4.5 and 4.6, respectively.

$$T_{T_t} = \frac{\sqrt{\overline{\left(T_t'\right)^2}}}{\overline{T_t}} \tag{4.5}$$

$$T_{P_t} = \frac{\sqrt{\overline{\left(P_t'\right)^2}}}{\overline{P_t}} \tag{4.6}$$

T_t' and P_t' are the fluctuating total temperature and pressure, respectively. $\overline{T_t}$ and $\overline{P_t}$ are the mean total temperature and pressure, respectively, averaged over 1000 data points (50 ms). T_{T_t} and T_{P_t} are the total temperature and pressure turbulence intensities, respectively.

4.4 Downstream Total Pressure

Because the exit flow is supersonic, a bow shock is present in front of the aspirating probe (see Figure 4-2).

Figure 4-2 Probe Bow Shock

This shock has no effect on the total temperature measured, but the total pressure measured is less than the actual total pressure upstream of the shock.

Since the static pressure is known upstream of the shock, the Mach number upstream of the shock can be calculated (Equation 4.7). The static pressures are assumed to be constant over the data acquisition time period.

$$\frac{P_{t_{probe}}}{P} = \left\{\frac{\gamma+1}{2}M^2\right\}^{\frac{\gamma}{\gamma-1}}\left\{\frac{2\gamma}{\gamma+1}M^2 - \frac{\gamma-1}{\gamma+1}\right\}^{\frac{1}{1-\gamma}} \tag{4.7}$$

P and M are the static pressure and Mach number upstream of the shock, respectively. $P_{t_{probe}}$ is the total pressure downstream of the shock measured by the probe. Now that the Mach number is known the total pressure upstream of the shock can be found (Equation 4.8).

$$\frac{P_t}{P} = \left\{1+\frac{\gamma-1}{2}M^2\right\}^{\frac{\gamma}{\gamma-1}} \tag{4.8}$$

P_t is the total pressure upstream of the shock. The static temperature, static density, velocity, and mass flow rate can then all be calculated. All total pressure data downstream of the test section presented in this thesis are the total pressures the probe measures unless otherwise noted.

4.5 Heat Transfer Computation

Since the Mach number upstream of the bow shock is now known from Equation 4.7, the static temperature, static density, and velocity can be calculated using Equations 4.9 - 4.11.

$$\frac{T_t}{T} = 1 + \frac{\gamma - 1}{2} M^2 \tag{4.9}$$

$$P = \rho \cdot \Re \cdot T \tag{4.10}$$

$$T_t = T + \frac{u^2}{2C_p} \tag{4.11}$$

Since the distance the probe traverses and the upstream and downstream total temperatures are known, the mass flow rate and the total heat transfer rate can be calculated (Equations 4.12 and 4.13).

$$m = \rho \cdot A \cdot u \tag{4.12}$$

$$q = mC_p\left(T_{t_{upstream}} - T_{t_{downstream}}\right) \tag{4.13}$$

Finally, a spacially averaged heat transfer coefficient can be calculated by using the following equation:

$$q = \bar{h} A_{blade}\left(\overline{T}_{t_{upstream}} - \overline{T}_{t_{blade}}\right) \tag{4.14}$$

where $\bar{h}$ is the average heat transfer coefficient.

4.6 Hot Wire Voltage Drift

Previous aspirating probes used platinum-tungsten hot wires. These wires can be operated at a maximum temperature of 300°C [13]. The actual wire operating temperature did not approach this value due to the problem of wire aging. However, platinum-iridium hot wires have a maximum operating temperature of 800°C [13]. For this experiment the wires were run in the 240°C to 380°C range.

For two subsequent runs under very similar conditions, the hot wire voltages were different. This was due to a drift in the DC voltage of the hot wires. The voltages from the first and second hot wires drifted 1.5 and 0.5 volts, respectively. This represents an approximate change of 60°C in temperature and 9 psi in pressure between the two runs. Since the upstream conditions measured by the other instrumentation were nearly the same, these changes in temperature and pressure are not correct. However, the general shape of the signals is the same. Therefore, the wires are still measuring the same changes in pressure and temperature.

A possible explanation involves the solder used to mount the hot wires. Since the wires are operating at higher temperatures, the solder used to mount the wires could be melting on to the wires causing the DC voltage to drift. Future probes will use a silver based solder which has a much higher melting temperature. The remaining data in the thesis was taken with each set of wires immediately following their calibration, before they had a chance to drift.

5.0 Results and Discussion

5.1 Data Presentation

As was previously mentioned in Chapter 3, for each signal (i.e. wire 1, wire 2, Kulite, and LVDT) 256,000 data points were collected for each run. This presents a difficulty in presenting the data in graphical form. It is difficult to plot all of the points on one plot. Therefore, a moving time average is done in order to reduce the data to graphical form. All graphs presented are averaged over 1000 data points (50ms or 0.015 inches). This is to see the overall shapes of the signals. However, when looking at the fluctuating components, i.e. turbulence intensities, all data points are used and the RMS is taken over each 1000 point segment.

Typically the reduced data from the high frequency probe captures the correct shape of the signal, but the DC level is inaccurate. Therefore, the total pressure data was DC shifted to a maximum value of 0.985 (the maximum expected to be seen due to the blade shock structures) and the total temperature ratio data was DC shifted to a maximum value of 1.0.

5.2 Power Spectra

Power spectra were calculated to see if the core or wake flow had any dominant frequencies. In Figure 5-1, the power spectra of the total pressure calculated using two hot wire voltages is shown for the core flow with 7.5% upstream turbulence. The amplitude is higher in the wakes due to higher fluctuations in flow pressure. The highest peaks are at 60Hz and 1000 Hz. The 60 Hz spike can be attributed to electronic noise. Figure 5-2 shows similar results for the total temperature. The 1000 Hz spike is probably associated with the characteristic frequency of the aspirating channel. The 1000 Hz spike is not present in Figure 5-3 which shows the total pressure data for the same run reduced from the Kulite transducer. The only spikes in this spectra are at harmonics and subharmonics of 60 Hz. Higher frequency spikes were expected on the Kulite power spectrum. These power spectra do not show any other dominant frequencies in the flow.

5.3 Kulite vs. Two Wire Data Reduction

If the Kulite pressure transducer is used, its signal can be converted directly into total pressure. Using this total pressure, only one wire is needed to find the total temperature by solving Equation 3.2. Figure 5-4 shows the results of using the two different means for determining the total pressure. Frequently, in reducing data of this nature by using the two different techniques, there is a large difference in the signal shapes [5,14]. However,

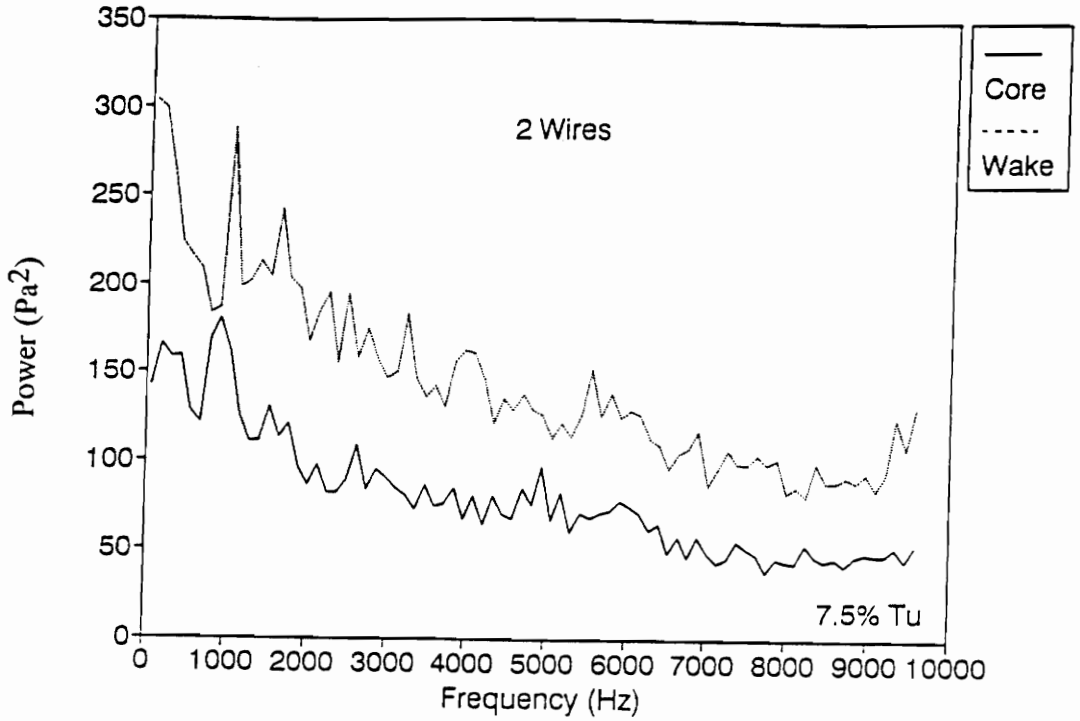

Figure 5-1 Total Pressure Power Spectrum (2 Wires)

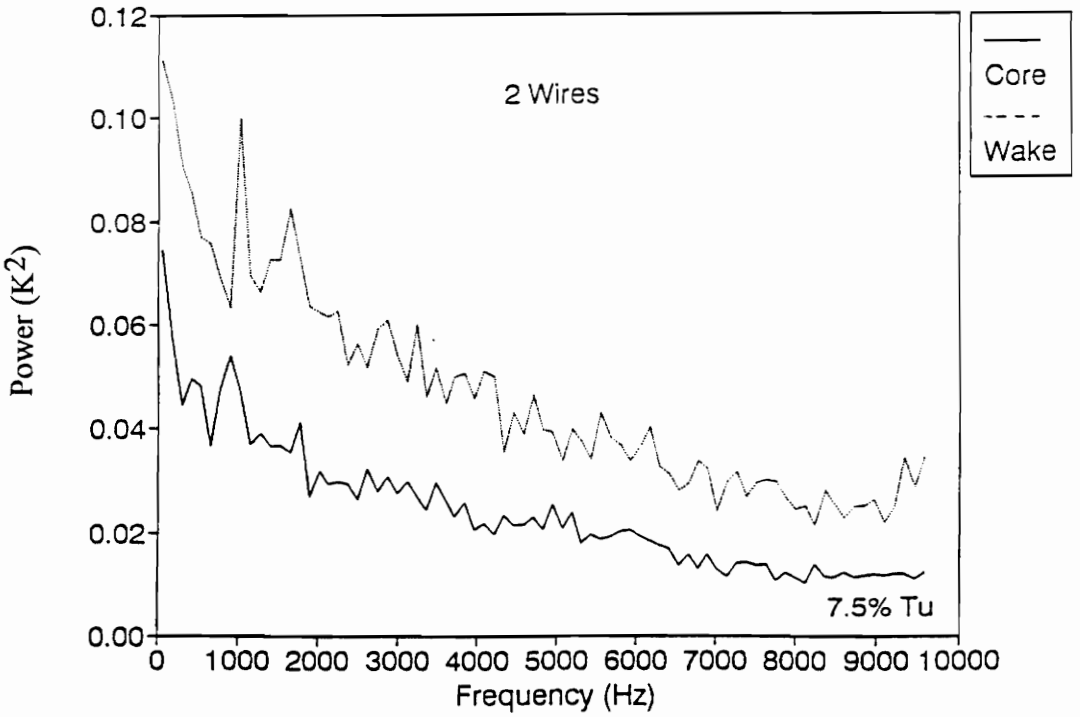

Figure 5-2 Total Temperature Power Spectrum (2 Wires)

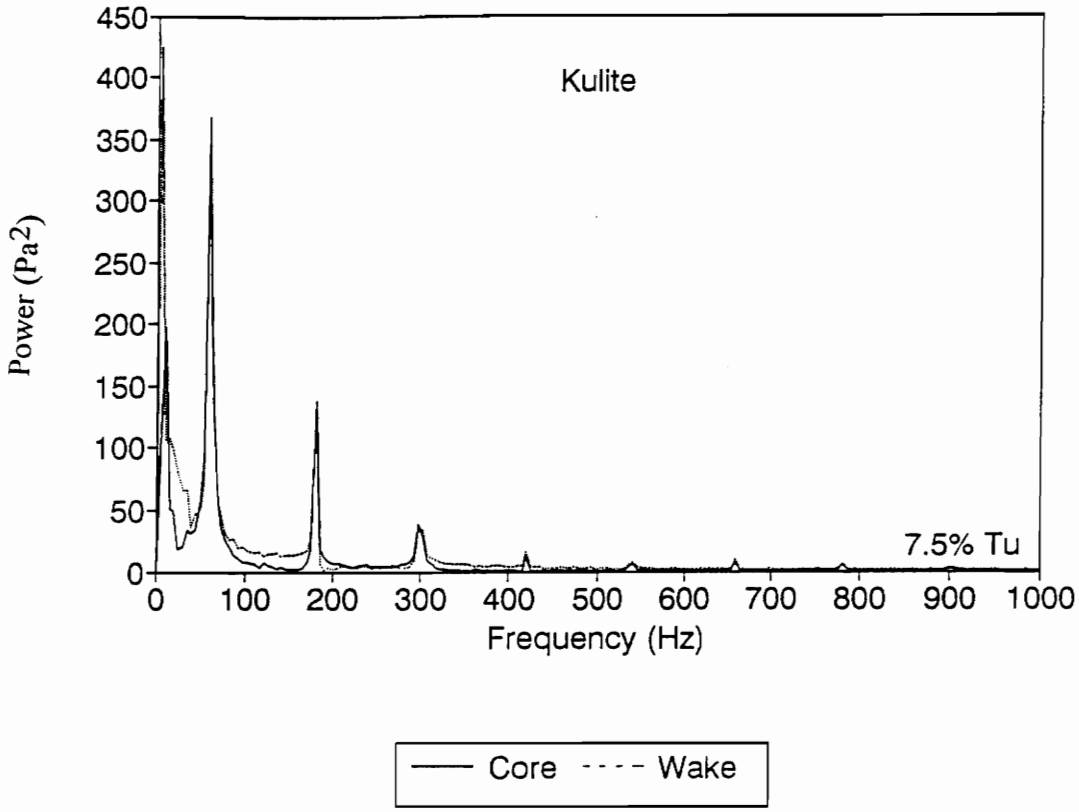

Figure 5-3 Total Pressure Power Spectrum (Kulite)

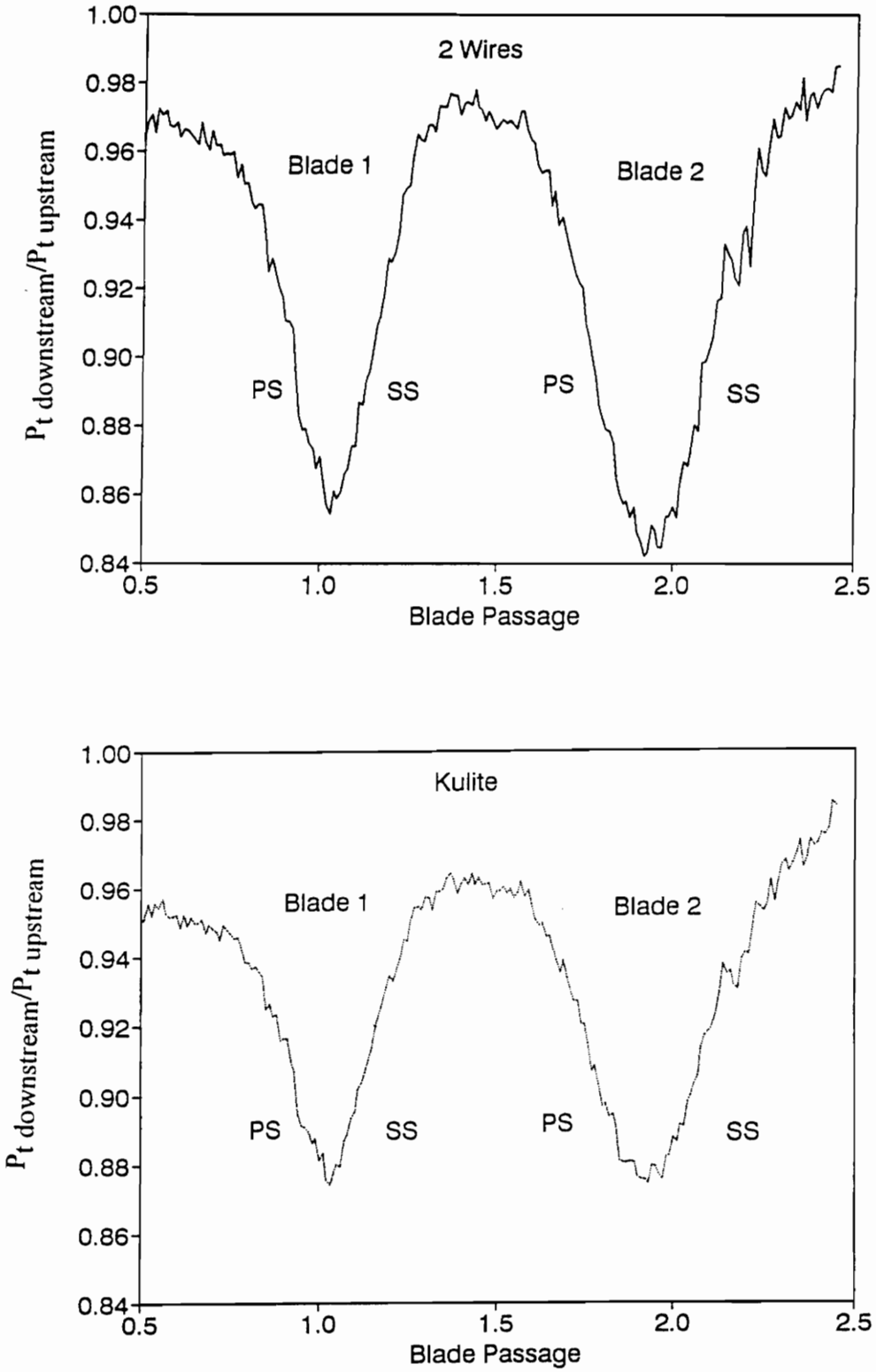

Figure 5-4 Total Pressure Ratio (Kulite vs. 2 Wires)

in this case the signals are amazingly similar. The Kulite signal's wakes are not quite as deep, but the general shapes are the same.

For the total temperature ratio data, the upward linear trend of the signal has been removed to better show the thermal wake structures. Figure 5-5 shows results for the total temperature results. Using the Kulite results in a shallower thermal wake, but again, the general shapes of the traces are similar. Since this is the case, the remaining data will be reduced by using the two hot wire voltages.

5.4 Total Pressure Ratio and Blade Losses

For each run, the probe was traversed from the core between the lower and center cooled blades through two complete blade passages. The hot wire voltages were reduced into total pressure downstream of the bow shock and total temperature. Using Equations 4.7 and 4.8 the total pressure in front of the probe bow shock was calculated. This value was divided by the upstream total pressure. The results were DC shifted to a maximum value of 0.985 which is the highest value of total pressure ratio expected to be seen due to the shock structure of the blade row.

Figure 5-6 compares the results for the two freestream turbulence levels. The blade pressure wake is very prominent as the probe traverses. The total pressure ratio varied by approximately 16% from the core to the wake region. The difference in upstream turbulence level does not seem to impact the total pressure ratio. The general curve shapes are very similar.

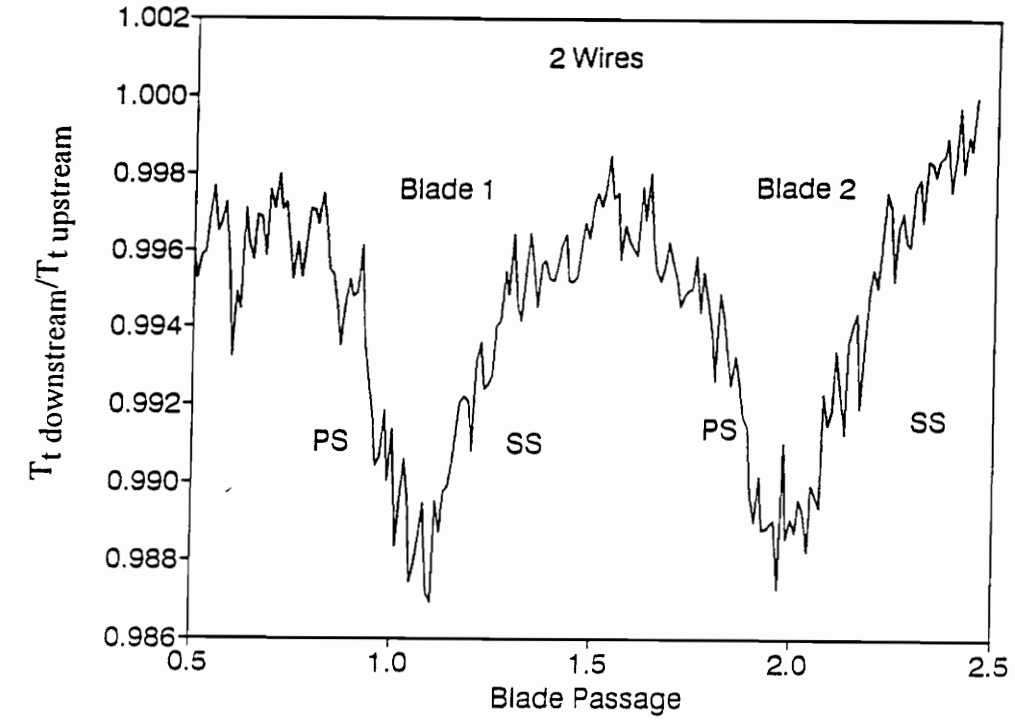

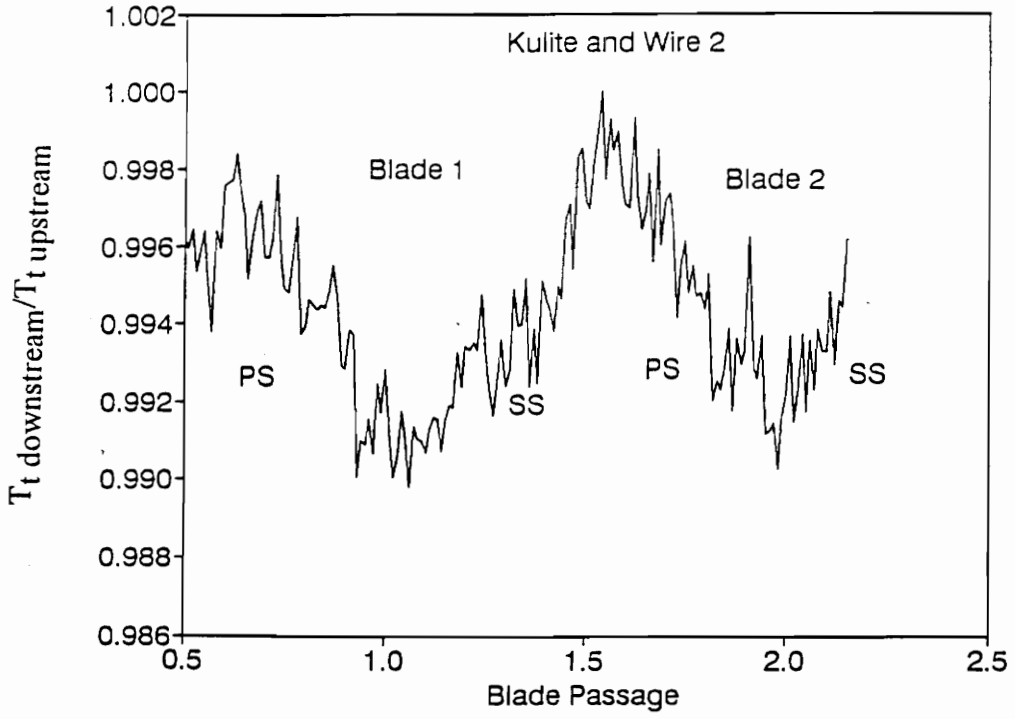

Figure 5-5 Total Temperature Ratio (Kulite vs. 2 Wires)

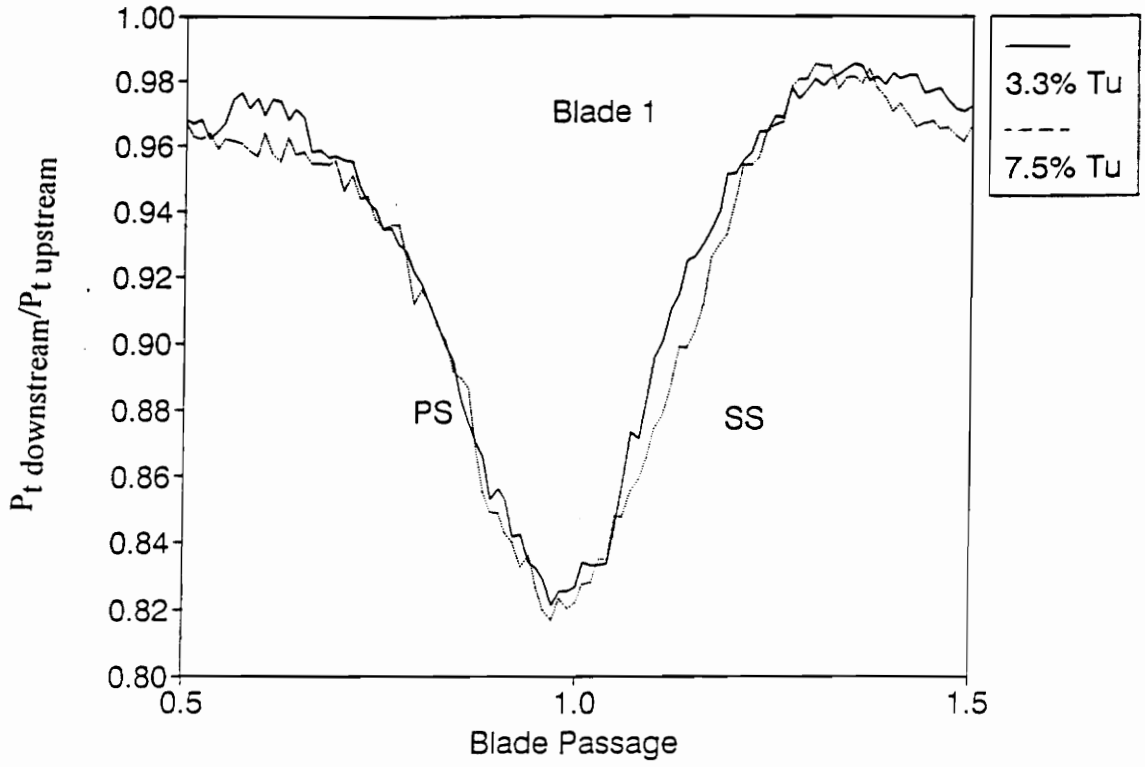

Figure 5-6 Total Pressure Ratio (3.3% T_u vs. 7.5% T_u)

Loss coefficients were calculated and the two only differed by 0.65% (7.56% for the 3.3% freestream turbulence intensity, 6.91% for the 7.5% freestream turbulence intensity). This small difference suggests that the freestream turbulence level has no effect on the blade losses.

5.5 Total Temperature Ratio and Heat Transfer

The total temperature ratio is defined as the downstream total temperature divided by the upstream total temperature. The upstream total temperature was measured with an exposed Type K thermocouple with a 5 mil bead diameter. The aspirating probe was used to measure the downstream total temperature. Hot wire probes are traditionally well suited for measuring fluctuations in flow parameters. However, the DC levels measured by the probe are typically inaccurate [14]. The total temperature ratio should have a value near one in the core regions. When originally calculating this parameter, it was sometimes greater than one or much less than one in the core. Therefore, the data presented was DC shifted in order to facilitate heat transfer rate calculations. The total temperature ratio also had an increasing trend over time. This linear trend was also removed from the data to more clearly show the thermal wakes.

The total temperature ratio for the two different upstream turbulence levels is shown in Figure 5-7. The two traces are very similar in shape and magnitude. Since all of the properties can be calculated downstream of the blade, a total heat transfer rate was computed. The total heat transfer rate for

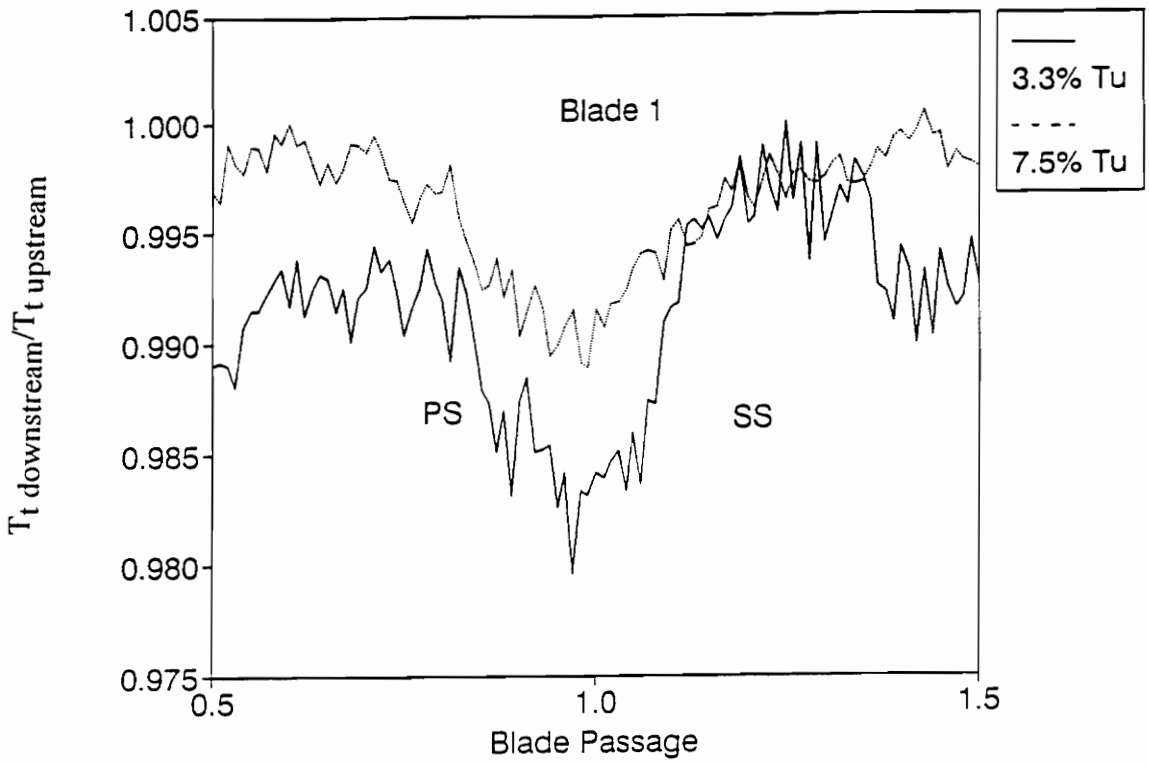

Figure 5-7 Total Temperature Ratio (3.3% T_u vs. 7.5% T_u)

the lower freestream turbulence intensity was 1.5% higher than the higher turbulence intensity case (1583 W for the 3.3% T_u, 1338 W for the 7.5% T_u). The corresponding average heat transfer coefficients were 2650 W/m^2 K for the 3.3% T_u and 2300 W/m^2 K for the 7.5% T_u. These values of the heat transfer coefficients were higher than expected by about a factor of three. For higher turbulence levels there should have been more heat transfer into the blades. However, the two runs were not identical and therefore cannot necessarily be compared. The upstream total temperatures were slightly different and the cooling rate of the blades might have also been different. These two effects play important roles in the heat transfer rates. Therefore, it is recommended that more testing be done with tighter controls on the tunnel heating and blade cooling before any heat transfer conclusions are drawn.

5.6 Turbulence Intensities

Turbulence intensity is a good way to compare the fluctuating portions of the flow parameters because it is normalized with the mean of the flow property. Equations 4.5 and 4.6 were used to calculate the total temperature and pressure turbulence intensities, respectively.

Figure 5-8 depicts the total pressure turbulence intensities for a run with each upstream turbulence intensity level. The first point to note is that the turbulence intensities in both cases are higher in the blade wake than in the core flow. This was expected because the boundary layer mixing effects should cause the flow to be more turbulent in the blade wakes. Also of

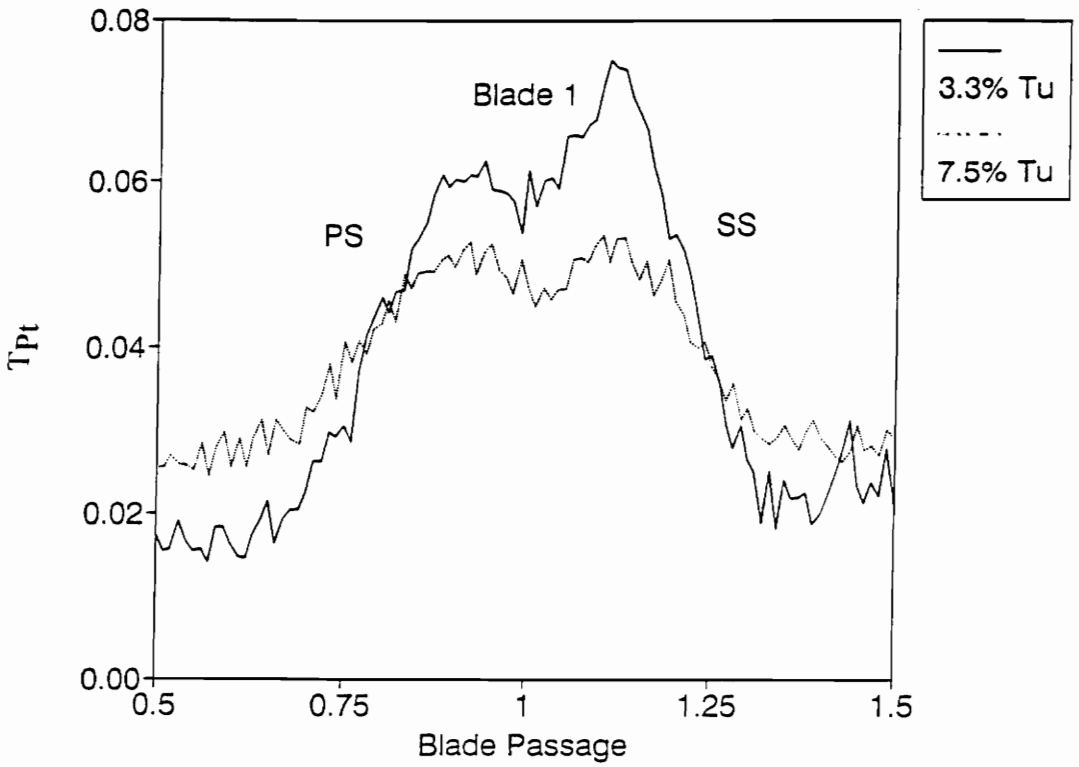

Figure 5-8 Total Pressure Turbulence Intensity

importance is the dip in turbulence intensity near the center of the blade wake. As the boundary layers from the pressure side and suction side mix in a free shear layer, there is a region between the two that has zero velocity. If the probe were closer to the trailing edge of the blades, this local dip would not be present and if the probe were moved further downstream, this dip would level out.

Finally, there is a noticeable difference between the turbulence intensity levels in the wake for the different upstream turbulence levels. With 3.3% upstream turbulence intensity, the total pressure turbulence level is 2% higher than for the 7.5% upstream turbulence intensity level. A possible reason given earlier was the influence of the upstream turbulence on the boundary layer [15]. Since the upstream turbulence with the presence of a turbulence screen is higher, the blade boundary layer is more fully turbulent. This flow is much more stable than with no screen. With no screen present, the flow over the blades transitions from laminar to turbulent. It is possible that this inherent instability could interact with the blade shock structures (see Figure 5-9) and result in a higher total pressure turbulence intensity.

The total temperature turbulence intensities for the same two runs are shown in Figure 5-10. The same general trends that were observed in the total pressure turbulence intensities are present here. The turbulence is higher in the wake, as before. Also as previously seen, a local dip in turbulence intensity is present in the center of the blade wake. The turbulence intensity level is again much higher with a lower freestream turbulence intensity

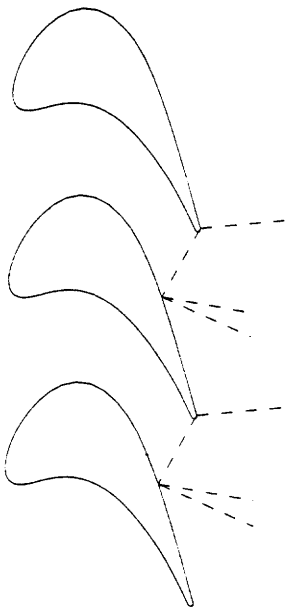

Figure 5-9 Blade Shock Structure

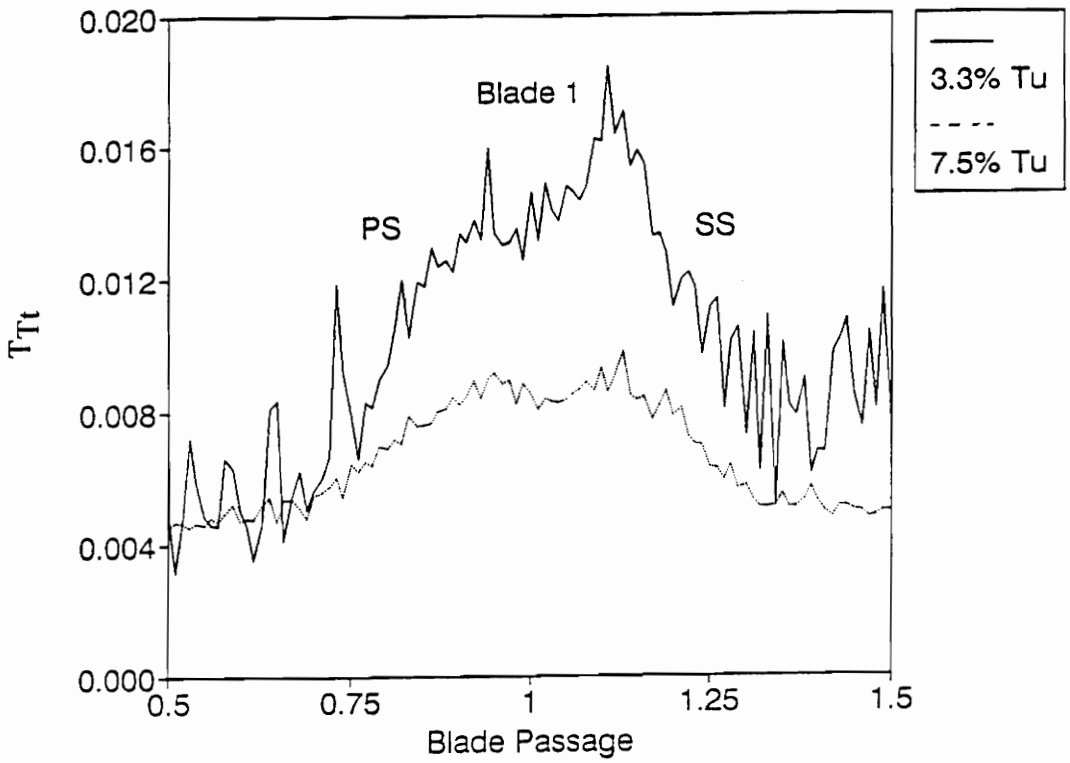

Figure 5-10 Total Temperature Turbulence Intensity

level. The turbulence intensity levels between the pressure and temperature plots are significantly different. That is because there is much less temperature fluctuation than pressure fluctuation in the flow.

6.0 Conclusions and Recommendations

A high frequency response dual hot wire aspirating probe was used to take measurements in the wake of a transonic turbine cascade. The incoming flow was heated and the blades were cooled to provide freestream to blade temperature ratios between 1.3 and 1.4. The freestream turbulence level was varied with the use of an upstream turbulence screen. The total temperature and total pressure turbulence intensities were computed, and with the use of other instrumentation, total temperature and total pressure ratios were calculated.

Several conclusions are able to be drawn from this research. The first is that the aspirating probe was able to measure the thermal and pressure wakes as it traversed through two blade passages. There was concern that the probe would not be able to perform in the high temperature environment experienced in the heated test section. However, the probe did perform as predicted. The results reduced from the two hot wires and Kulite pressure transducer were similar.

By measuring total temperature and total pressure turbulence intensities, it is evident that there was more downstream property fluctuation

in the wakes with the lower upstream turbulence level. The cause of this result is not certain and must be further researched.

Based on the data from this experiment, it is also concluded that the freestream turbulence level has no effect on the total pressure losses of the blades.

Recommendations for future research:

1. Use a silver based solder to prevent the solder from melting on to the hot wires and causing DC drift.
2. Repeat the measurements for higher freestream turbulence intensity levels to see if the aforementioned trends continue.
3. Take shadowgraphs of the flow over the blades to visually see the differences in blade boundary layer structures.
4. Use the probe to measure the effects of multiple shock passages through the blade row.

Appendix A

Non-normalized total pressure and temperature data

This appendix presents plots of total temperature and total pressure for each freestream turbulence level. The data presented are not normalized with their corresponding upstream measurements nor are they offset or otherwise conditioned.

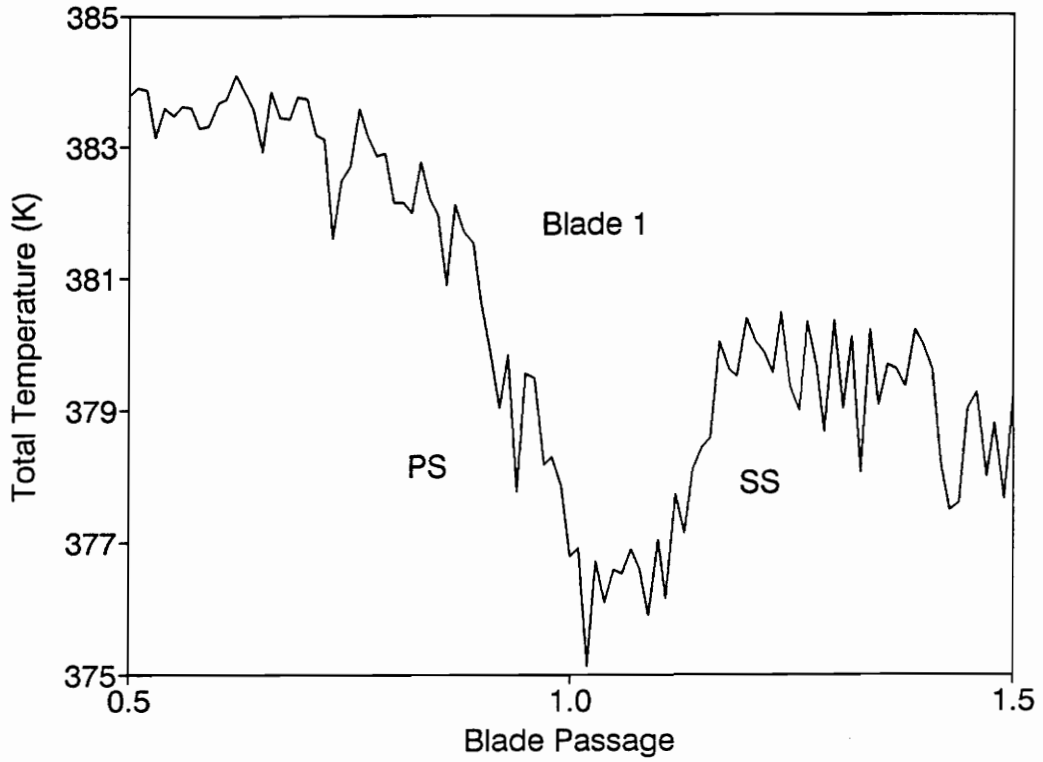

Figure A-1 Total Temperature, 3.3% T_u

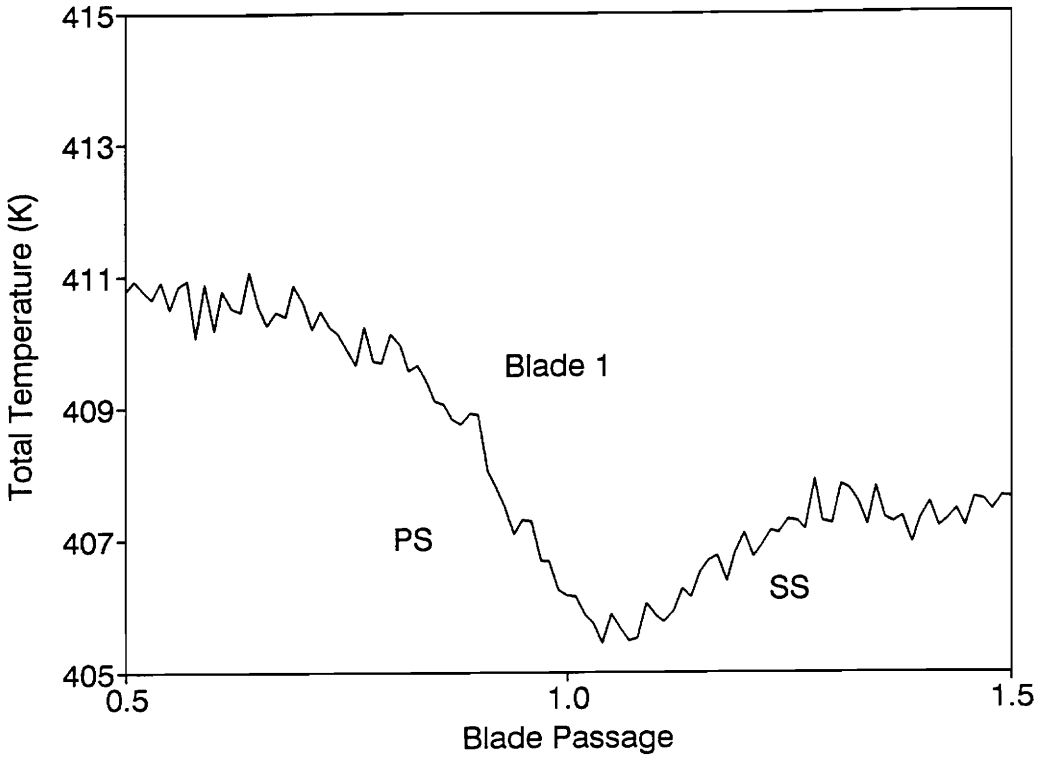

Figure A-2 Total Temperature, 7.5% T_u

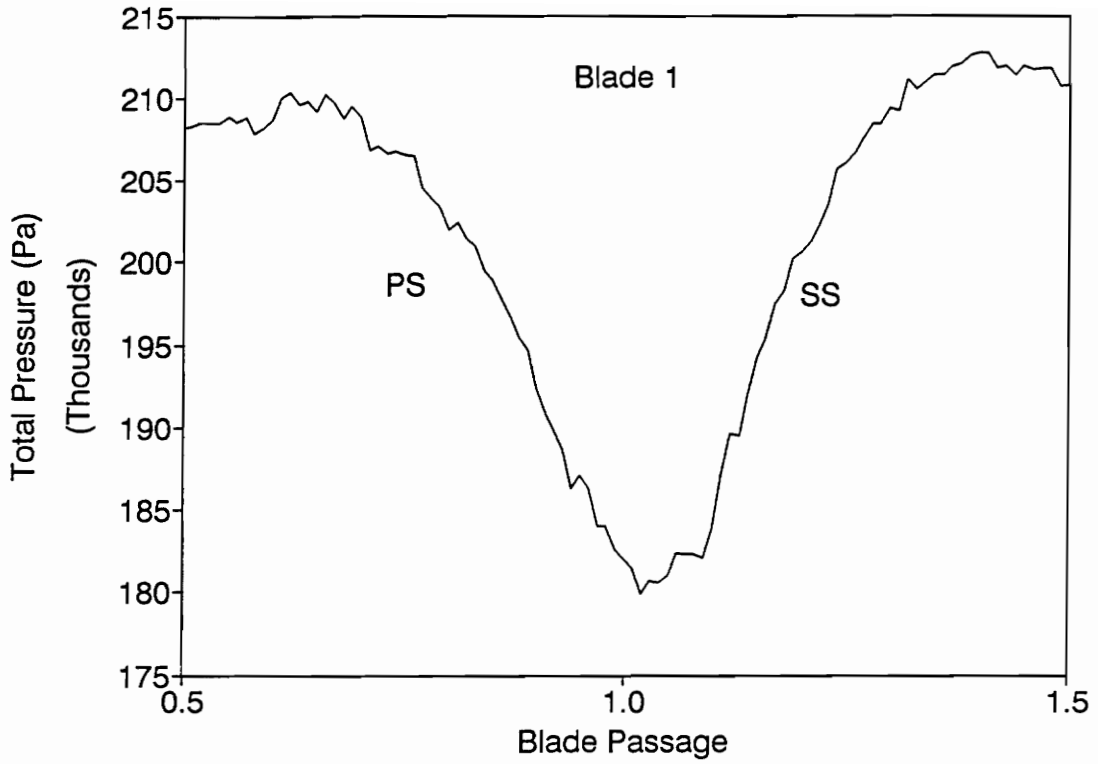

Figure A-3 Total Pressure, 3.3% T_u

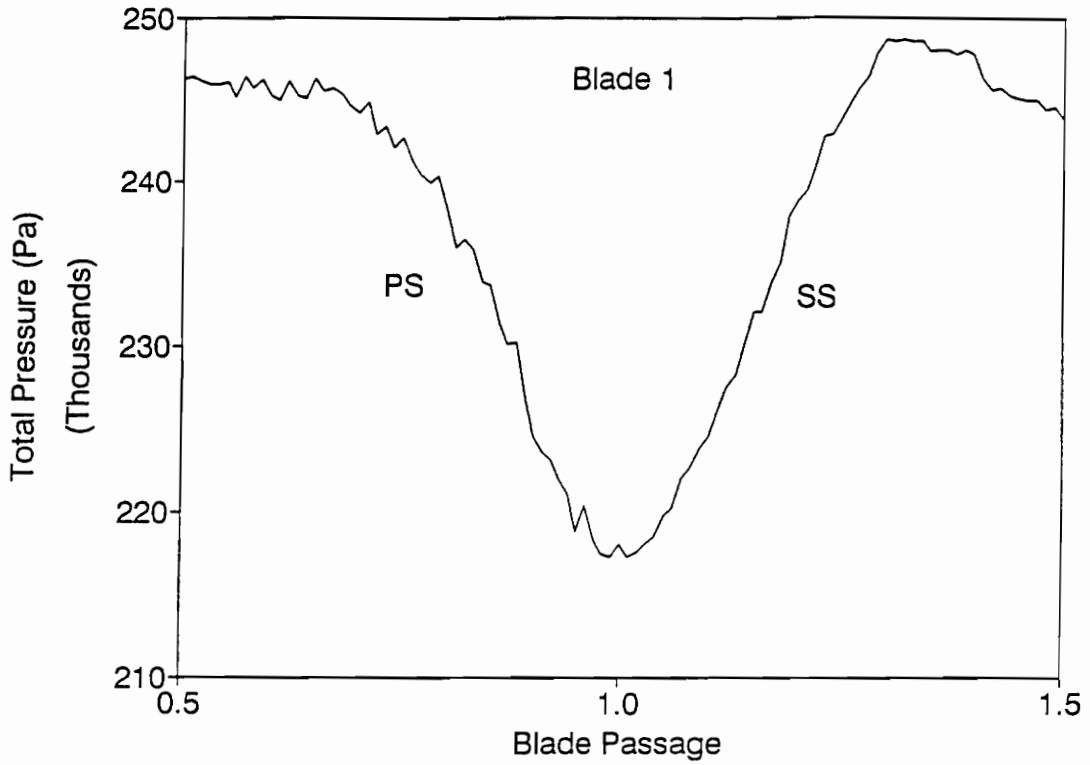

Figure A-4 Total Pressure, 7.5% T_u

References

1. Ng, W. F., Epstein, A.H., "A High Frequency Temperature and Pressure Probe for Unsteady Compressible Flows," *Review of Scientific Instruments*, Vol 54, No. 12, December 1983.

2. Ng, W.F., "Review - Simultaneous Measurements of Stagnation Temperature and Pressure Using an Aspirating Probe," International Symposium on Pressure and Temperature Measurements, ASME Winter Annual Meeting, December 1986, Anaheim, CA.

3. Osborne, D.J., "Time-Resolved Measurements of a Transonic Compressor During Surge and Rotating Stall," Master of Science Thesis, Department of Mechanical Engineering, Virginia Polytechnic Institute, August 1992.

4. Ninnemann, T.A., "Aspirating Probes for Measurement of Mean Concentration and Fluctuating Quantities in Supersonic Air/Helium Shear Layers," Master of Science Thesis, Department of Mechanical Engineering, Virginia Polytechnic Institute, December 1990.

5. Van Zante, D.E., Suder, K.L., Strazisar, A.J., Okiishi, T.H., "An Improved Aspirating Probe For Total-Temperature and Total-Pressure Measurements In Compressor Flows," International Gas Turbine and Aeroengine Conference and Exposition, The Hague, Netherlands, June 1994.

6. Moss, R.W., and Oldfield, M.L.G., "Effect of Free-Stream Turbulence on Flat-Plate Heat Flux Signals: Spectra and Eddy Transport Velocities," International Gas Turbine and Aeroengine Conference and Exposition, The Hague, Netherlands, June 1994.

7. Gundappa, M. and Diller, T.E., "The Effects of Free-Stream Turbulence and Flow Pulsation on Heat Transfer From a Cylinder in Crossflow," ASME Winter Annual Meeting, Miami Beach, Florida, November 1985.

8. Glezer, B., Moon, H.K., Zhang, L., Camci, C., "Application of a Heat Flux/Calorimeter-Based Method to Assess the Effect of Turbulence on Turbine Airfoil Heat Transfer," International Gas Turbine and Aeroengine Congress and Exposition, The Hague, Netherlands, June 1994.

9. Maciejewski, P.K., Rivir, R.B., "Effects of Surface Riblets and Free-Stream Turbulence on Heat Transfer in a Linear Turbine Cascade," International Gas Turbine and Aeroengine Congress and Exposition, The Hague, Netherlands, June 1994.

10. Bertsch, R., "An Experimental Examination of the Influence of Trailing Edge Coolant Ejection on Blade Losses in Transonic Turbine Cascades," Master of Science Thesis, Department of Mechanical Engineering, Virginia Polytechnic Institute, 1990.

11. Johnson, L., Research Assistant, Virginia Polytechnic Institute and State University, Blacksburg, VA, Personal Communication, July 1994.

12. Kotidis, P.A., "Unsteady Radial Transport in a Transonic Compressor Stage," Gas Turbine Laboratory, Massachusetts Institute of Technology, Cambridge, MA, September 1989.

13. TSI Incorporated, "Hot Wire / Hot Film Anemometry Probes and Accessories," 1988.

14. Ng, W.F., Professor, Virginia Polytechnic Institute and State University, Blacksburg, VA, Personal Communication, July 1994.

15. Hancock, P.E., Bradshaw, P., "The Effect of Free-Stream Turbulence on Turbulent Boundary Layers," *Transactions of the ASME Journal of Fluids Engineering*, Vol 105, p284-289, 1983.

Vita

The author was born in Natrona, Pennsylvania on October 30, 1970. He graduated as salutatorian of Butler High School in 1989. In the summer of 1992, he spent six weeks at Edwards Air Force Base working at the Phillips Laboratory. In 1993, he graduated with a Bachelor of Science degree in aeronautical engineering as a distinguished graduate from the United States Air Force Academy. That same year he was commissioned a second lieutenant in the United States Air Force and was admitted to Virginia Polytechnic Institute and State University. Following the completion of his Master of Science degree, the author will enter Undergraduate Pilot Training in August 1994.

Alexis Mezynski